

# Beneficial effects of PGC-1 $\alpha$ in the substantia nigra of a mouse model of MPTP-induced dopaminergic neurotoxicity

Yingqing Wang<sup>1,\*</sup>, Chun Chen<sup>1,\*</sup>, Wanling Huang<sup>1</sup>, Maoxin Huang<sup>2</sup>, Juhua Wang<sup>1</sup>, Xiaochun Chen<sup>1,3</sup>, Qinyong Ye<sup>1,3</sup>

<sup>1</sup>Department of Neurology, Fujian Institute of Geriatrics, The Affiliated Union Hospital of Fujian Medical University, Fuzhou, Fujian, China

<sup>2</sup>Clinical Medicine, Xiangya School of Medicine, Central South University, Changsha, Hunan, China

<sup>3</sup>Key Laboratory of Brain Aging and Neurodegenerative Diseases, Fujian Key Laboratory of Molecular Neurology, Fujian Medical University, Fuzhou, China

\*Equal contribution and co-first authors

**Correspondence to:** Qinyong Ye; email: [unionqyye@163.com](mailto:unionqyye@163.com)

**Keywords:** Parkinson's disease, C57BL mice, mitochondria, MPTP, PGC-1 $\alpha$

**Received:** November 12, 2018

**Accepted:** October 5, 2019

**Published:** October 21, 2019

**Copyright:** Wang et al. This is an open-access article distributed under the terms of the Creative Commons Attribution License (CC BY 3.0), which permits unrestricted use, distribution, and reproduction in any medium, provided the original author and source are credited.

## ABSTRACT

**Background:** Mitochondrial dysfunction and oxidative stress are closely associated with the pathogenesis of Parkinson's disease. Peroxisome proliferator-activated receptor  $\gamma$  coactivator 1 alpha (PGC-1 $\alpha$ ) is thought to play multiple roles in the regulation of mitochondrial biogenesis and cellular energy metabolism. We recently reported that altering PGC-1 $\alpha$  gene expression modulates mitochondrial functions in N-methyl-4-phenylpyridinium ion (MPP<sup>+</sup>) treated human SH-SY5Y neuroblastoma cells, possibly via the regulation of Estrogen-related receptor  $\alpha$  (ERR $\alpha$ ), nuclear respiratory factor 1 (NRF-1), nuclear respiratory factor 2 (NRF-2) and peroxisome proliferator-activated receptor  $\gamma$  (PPAR $\gamma$ ) expression. In the present study, we aimed to further investigate the potential beneficial effects of PGC-1 $\alpha$  in the substantia nigra of 1-methyl-4-phenyl-1,2,3,6-tetrahydropyridine (MPTP) treated C57BL mice.

**Methods:** The overexpression or knockdown of the PGC-1 $\alpha$  gene in the mouse model of dopaminergic neurotoxicity was performed using a stereotactic injection of lentivirus in MPTP-treated male C57BL/6 mice. Mice were randomly assigned to one of 6 groups (n=24 per group): normal saline (NS) intraperitoneal injection (i.p.) (con); MPTP i.p. (M); solvent of the lentivirus striatal injection (lentivirus control) + MPTP i.p. (LVcon+M); lentivirus striatal injection + MPTP i.p. (LV+M); LV-PGC-1 $\alpha$  striatum injection + MPTP i.p. (LVPGC+M); and LV-PGC-1 $\alpha$ -siRNA striatal injection + MPTP i.p. (LVsiRNA+M). Intraperitoneal injections of MPTP/NS were conducted two weeks after lentivirus injection.

**Results:** We found significant improvement in motor behavior and increases in tyrosine hydroxylase expression in the substantia nigra (SN) in the brains of mice in the LVPGC+M group. The opposite tendency was observed in those in the LVsiRNA+M group. The expression of superoxide dismutase (SOD) in the SN region was also consistent with the changes in PGC-1 $\alpha$  expression. Electron microscopy showed an increasing trend in the mitochondrial density in the LVPGC+M group and a decreasing trend in the M and LVsiRNA+M groups compared to that in the controls.

**Conclusions:** Our results indicated that PGC-1 $\alpha$  rescues the effects of MPTP-induced mitochondrial dysfunction in C57BL mice.

## INTRODUCTION

As the second most common adult-onset neurodegenerative disease next to Alzheimer's disease, idiopathic Parkinson's disease (PD) is characterized by  $\alpha$ -synuclein accumulation and the progressive loss of dopaminergic neurons in the human substantia nigra pars compacta (SNpc). The inhibition of the electron transport chain (ETC) and mitochondrial dysfunction have been implicated in the pathogenesis of PD. The first line of evidence was obtained from the description of ETC complex I (CI) deficiency in a postmortem study of PD [1, 2]. Neurotoxins, including 1-methyl-4-phenyl-1,2,3,6-tetrahydropyridine (MPTP) and rotenone, were found to inhibit CI activity [3]. Peroxisome proliferator-activated receptor  $\gamma$  (PPAR $\gamma$ ) coactivator 1 alpha (PGC-1 $\alpha$ ) is a key regulator of mitochondrial biogenesis and cellular energy metabolism in response to extracellular changes [4, 5]. Recent studies have highlighted important roles of PGC-1 $\alpha$  in neurodegenerative diseases. A genome-wide meta-analysis identified a general downregulation of PGC-1 $\alpha$ -responsive gene transcription in the SN of PD patients [6]. Increased neuron vulnerability to neurotoxicity [7] and loss of dopaminergic neurons [8] were found in PGC-1 $\alpha$  knockdown mice. The overexpression of PGC-1 $\alpha$  in mouse neurons also resulted in increased resistance against MPTP-induced nigrostriatal degeneration and ETC activity [9], suggesting the potential significance of PGC-1 $\alpha$  in the treatment of PD.

Our previous *ex vivo* study using adenovirus transfection to manipulate PGC-1 $\alpha$  gene expression in N-methyl-4-phenylpyridinium ion (MPP<sup>+</sup>) -treated neuroblastoma cells showed changes in several mitochondrial functions. These changes occurred in the mitochondrial membrane potential, ATP production, cytochrome C release, and H<sub>2</sub>O<sub>2</sub> production. The effects of PGC-1 $\alpha$ , manifesting as the regulation of downstream transcriptional factors, were also identified. Estrogen-related receptor  $\alpha$  (ERR $\alpha$ ) and nuclear respiratory factor 1 (NRF-1) were found to be the key co-factors in cellular protection [10, 11]. To shed further light on the therapeutic benefits of PGC-1 $\alpha$ , we investigated the effects of manipulating its expression in MPTP-treated C57BL mice in the present study. For bidirectional comparison, the lentivirus system was used both for PGC-1 $\alpha$  overexpression and knockdown, and the engineered lentivirus preparations were injected into the striatum to establish two types of mouse models. Using these models, we primarily focused on behavioral changes, dopaminergic neuron survival, and mitochondrial changes in the SN after MPTP treatment.

### Declarations

We used male C57BL/6 mice. All animal experiments were carried out under the guidelines of the Animal

Care and Use Committee of Fujian Medical University. The animal experimentation protocols were approved by the ethics review committee of Fujian Medical University.

## RESULTS

### LV-PGC-1 $\alpha$ and LV-PGC-1 $\alpha$ -siRNA were widely distributed in the SN region

To observe whether lentivirus was transmitted from the striatum to the substantia nigra, one week after infection, GFP was detected to prove successful lentivirus transfection. GFP fluorescence was observed in cells throughout the substantia nigra and striatum (Figure 1), which demonstrated that lentivirus could be transported from the striatum to the substantia nigra and successfully transfected into cells.

### Changes in PGC-1 $\alpha$ expression in the SN

To determine whether PGC-1 $\alpha$  was overexpressed or knocked down in the substantia nigra, we detected the protein and mRNA levels of PGC-1 $\alpha$  in the substantia nigra.

In the overexpression analysis, western blotting (Figure 2A, 2C) showed that PGC-1 $\alpha$  expression in the LVPGC+M group was 1.13 times higher than that in the LV+M group ( $P < 0.05$ ), while no differences were found between the M and con groups. Real-time PCR (Figure 2D) showed that PGC-1 $\alpha$  mRNA levels in the LVPGC+M group were 8.64 times higher than those in the LV+M group ( $P < 0.01$ ), and those of the M group showed no significant differences compared with those of the con group, which showed a consistently positive trend of protein expression. In the knockdown analysis, western blotting (Figure 2B, 2E) showed a significant reduction in PGC-1 $\alpha$  expression levels when treated with MPTP and LV-PGC-1 $\alpha$ -siRNA (M vs. con, 26.67%,  $P < 0.01$ ; LVsiRNA+M vs. LV+M, 62.72%,  $P < 0.01$ ). The same trend was found in the mRNA levels of PGC-1 $\alpha$  (Figure 2F) (M vs. con, 27.84%,  $P < 0.05$ ; LVsiRNA+M vs. LV+M, 73.12%,  $P < 0.01$ ). Thus, PGC-1 $\alpha$  was successfully overexpressed and knocked down in the mouse SN at both the protein and mRNA levels using our overexpression and siRNA PGC-1 $\alpha$  constructs. Additionally, MPTP could alter PGC-1 $\alpha$  expression levels, but not as much as the LV-PGC-1 $\alpha$  and LV-PGC-1 $\alpha$ -siRNA.

### PGC-1 $\alpha$ improves MPTP-induced behavioral abnormalities

A successful mouse model of MPTP-induced dopaminergic neurotoxicity is the basis for the next

experiment. The success of the model can be judged by the difference in behavior before and after modeling. The rotarod test is a widely used behavioral test used to assess balance and body coordination in mice [12, 13]. This test rapidly provides easily interpretable results for

investigators. The equipment is simple and easy to operate.

The time the mouse stayed on the rod was recorded and plotted against the correlated rotarod speed. The area

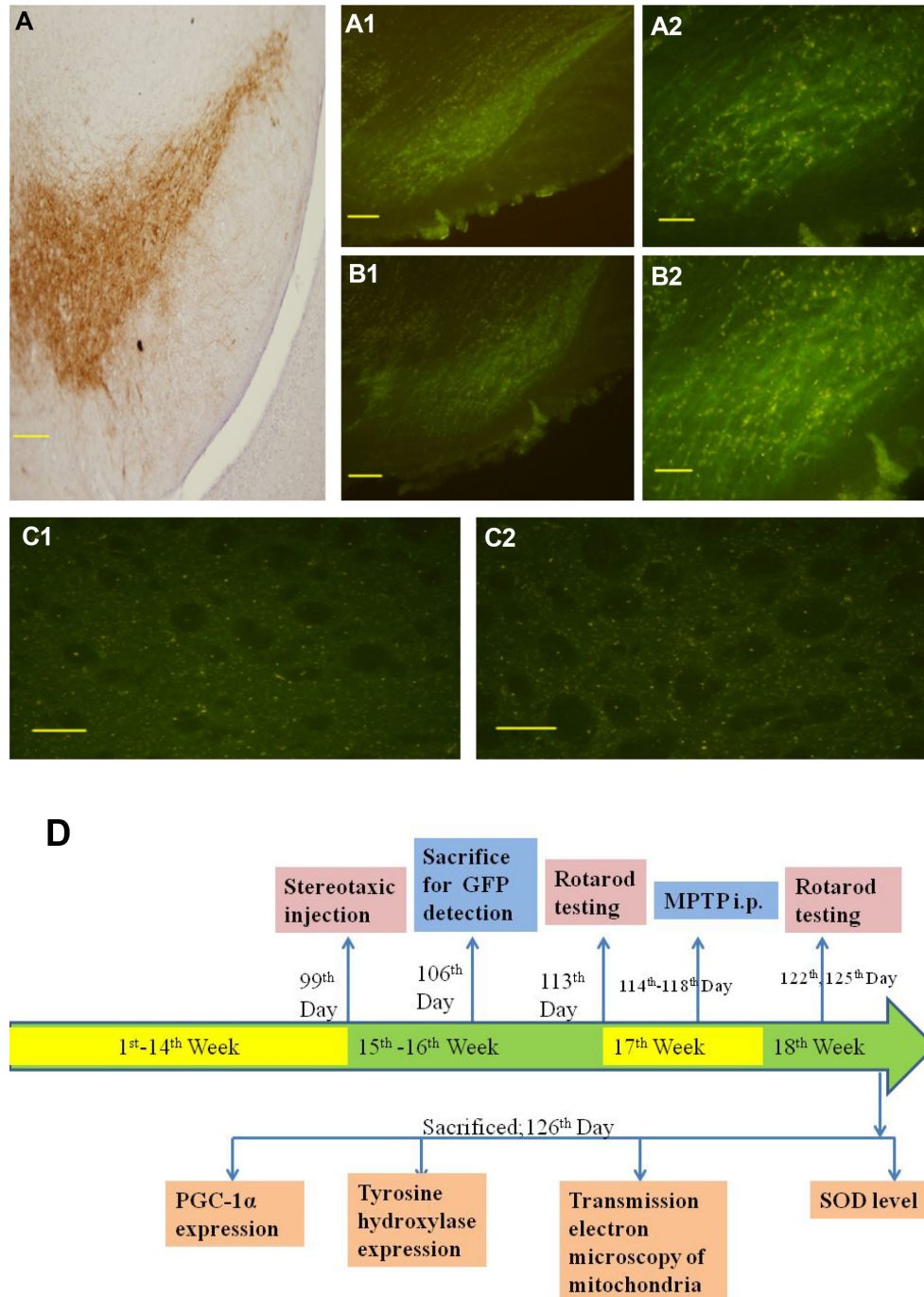


**Figure 1. Distribution of lentivirus in the SN, striatum region and the representative schematic.** (A) shows immunohistochemical staining of the substantia nigra in the control group. (A1 and A2) show successful LV-PGC-1 $\alpha$  infection in the substantia nigra of mice. (B1 and B2) show successful LV-PGC-1 $\alpha$ -siRNA infection of the substantia nigra of mice. (C1 and C2) show the striatum infected with LV-PGC-1 $\alpha$  and LV-PGC-1 $\alpha$ -siRNA, respectively. (D) shows a schematic representation of the experimental paradigm. Scale bar: 20  $\mu$ m. Magnification:  $\times$ 200 for A1, B1;  $\times$ 400 for A, A2, B2, C1, C2.

under the curve was calculated to represent the overall performance of individual mice (rotarod test scores). In the overexpression experiments, the results (Figure 3A) showed that three days after MPTP administration, the rotarod test scores of the M group, the LVcon+M group, and the LV+M group decreased by 15.30% ( $P < 0.01$ ), 17.14% ( $P < 0.05$ ), and 17.38% ( $P < 0.05$ ), respectively, compared with the scores on the day before MPTP administration. Comparing groups on the third day after MPTP administration showed that the performance of the M group decreased by 15.28% ( $P < 0.01$ ) compared with that of the con group, and the performance of the LVPGC+M group increased by 18% ( $P < 0.01$ )

compared with that of the LV+M group. In the knockdown experiment, the results (Figure 3B) showed that three days after MPTP administration, the rotarod test scores of the M group, the LVcon+M group, and the LV+M group decreased by 9.50% ( $P < 0.01$ ), 8.93% ( $P < 0.01$ ), 8.90% ( $P < 0.01$ ), respectively, compared with the scores on the day before MPTP administration. Comparing the groups on the third day after MPTP administration showed that the performance of the M group decreased by 9.43% ( $P < 0.01$ ) compared with that of the con group, and the performance of the LVsiRNA+M group decreased by 7.50% ( $P < 0.01$ ) compared with that of the LV+M group.

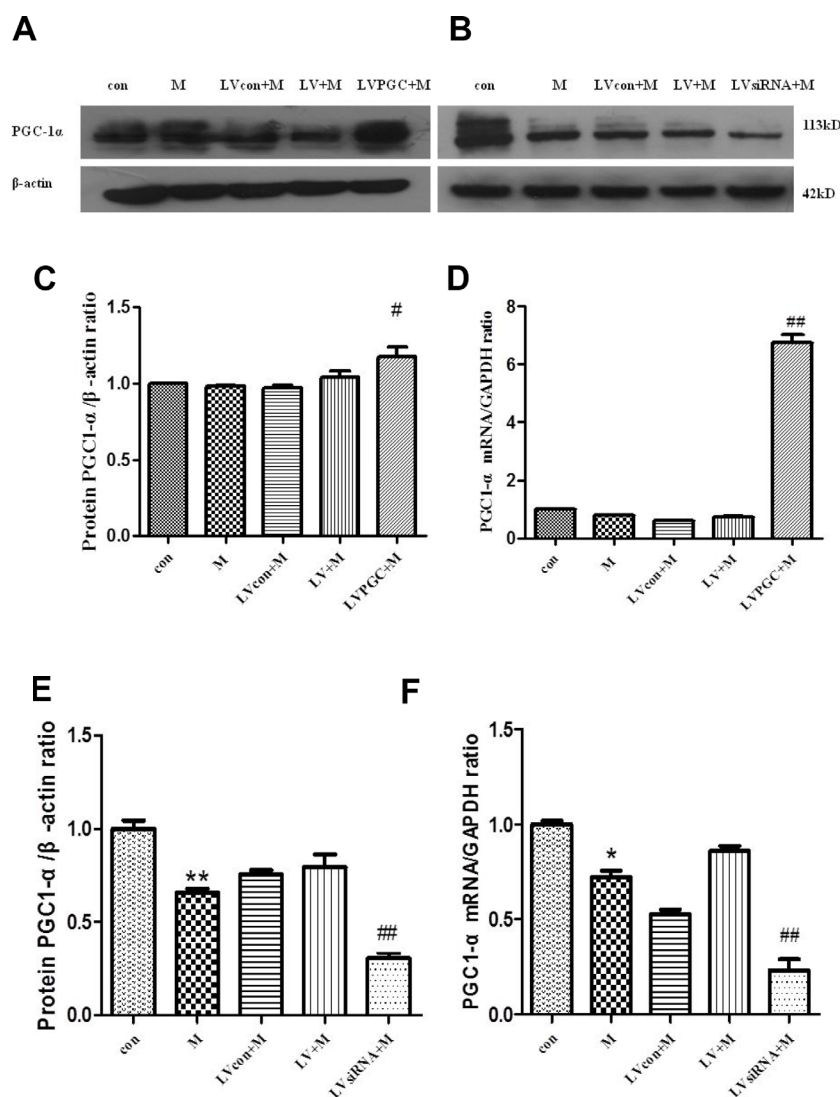


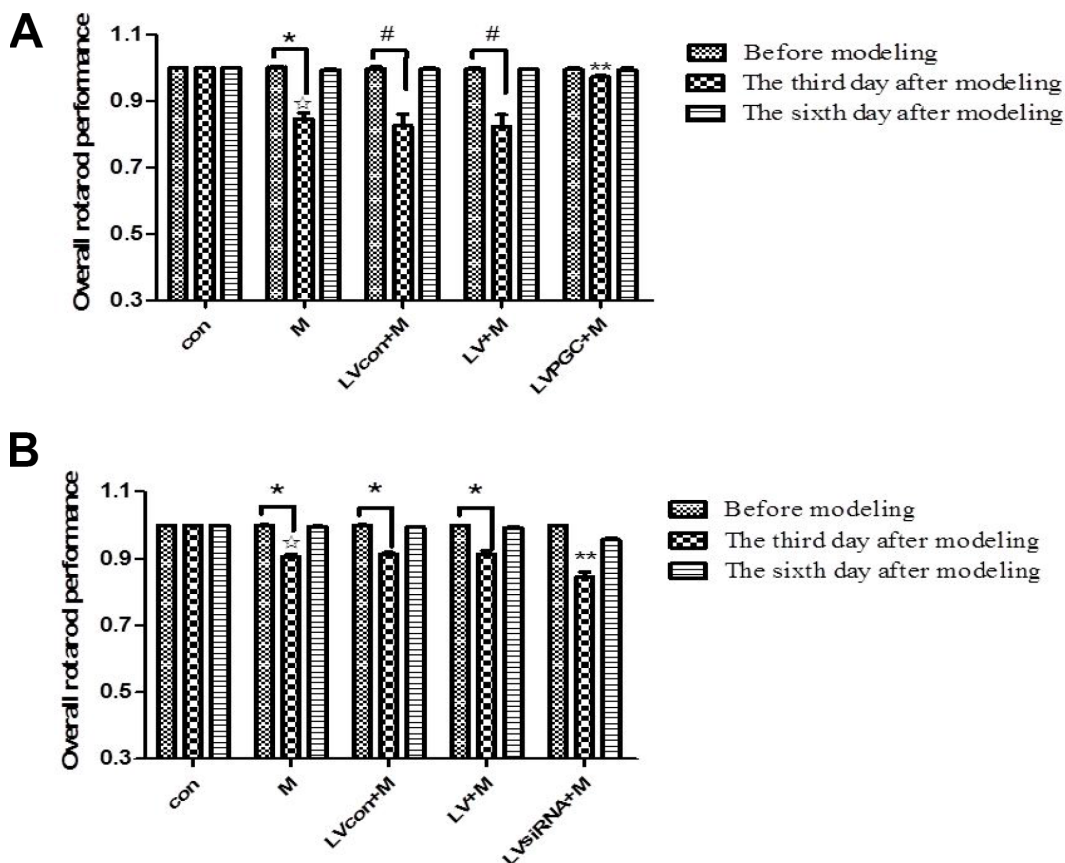
**Figure 2. Expression of PGC-1α in the SN of C57BL mice.** (A, B) PGC-1α protein expression patterns; (C, D) PGC-1α protein expression patterns after overexpression, detected using western blotting and real-time PCR; (E, F) PGC-1 α protein expression after knockdown, detected using western blotting and real-time PCR; Quantification of the results of three experiments are presented as the means ± SD. The groups were con (con group), M (MPTP group), LVcon+M (solvent of lentivirus+MPTP group), LV+M (lentivirus+MPTP group), LVPGC+M (LV-PGC-1α+MPTP group), LVsiRNA+M (LV-PGC-1αsiRNA+MPTP group); # $P < 0.05$ , ## $P < 0.01$  compared with the LV+M group, \*\* $P < 0.01$ , \* $P < 0.05$  compared with the con group.

### PGC-1 $\alpha$ attenuates MPTP-induced tyrosine hydroxylase loss in the mouse substantia nigra

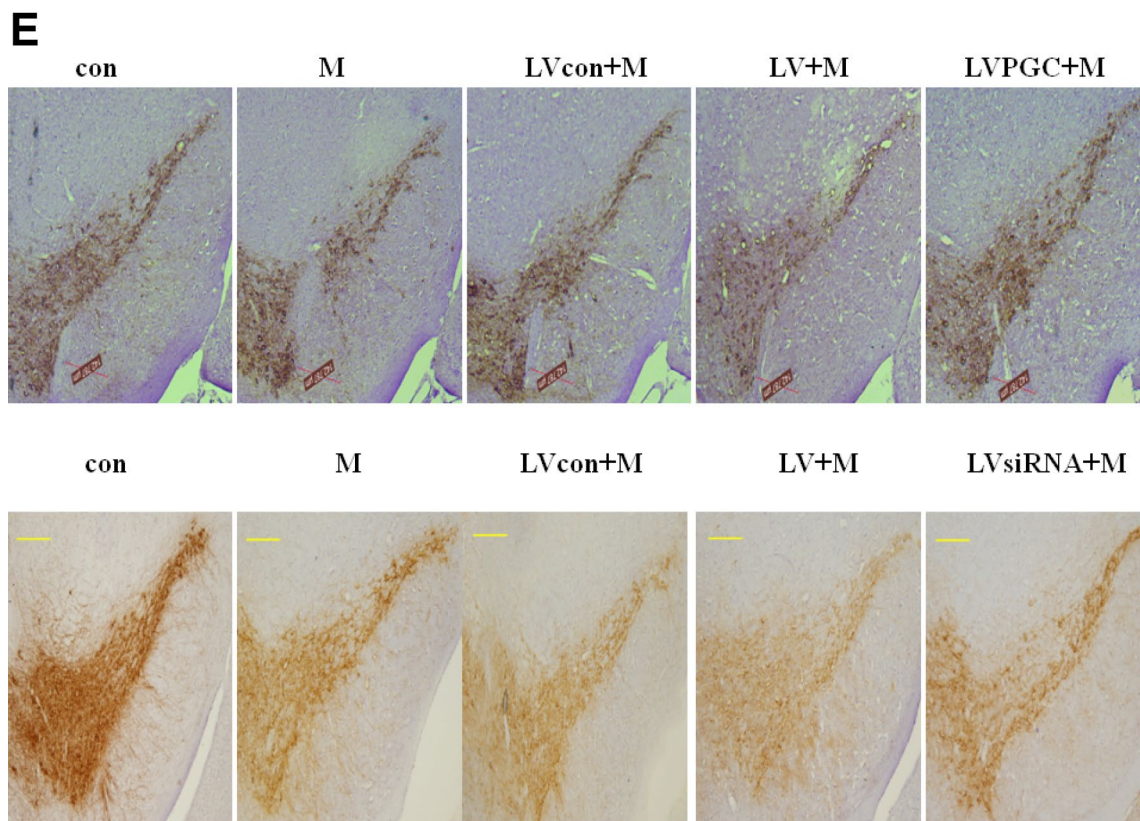
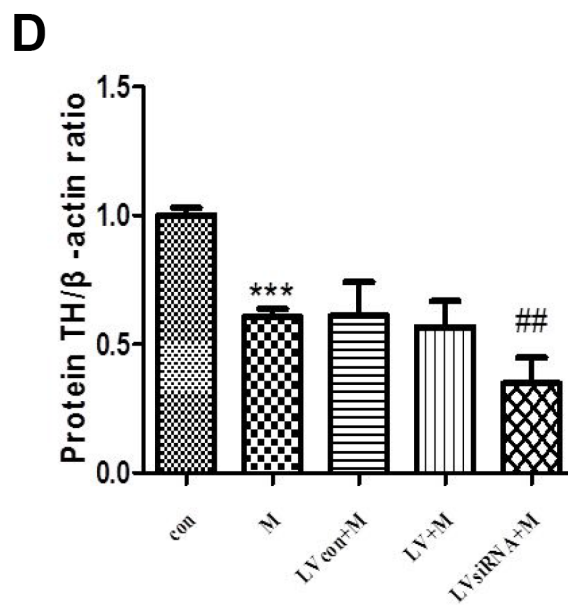
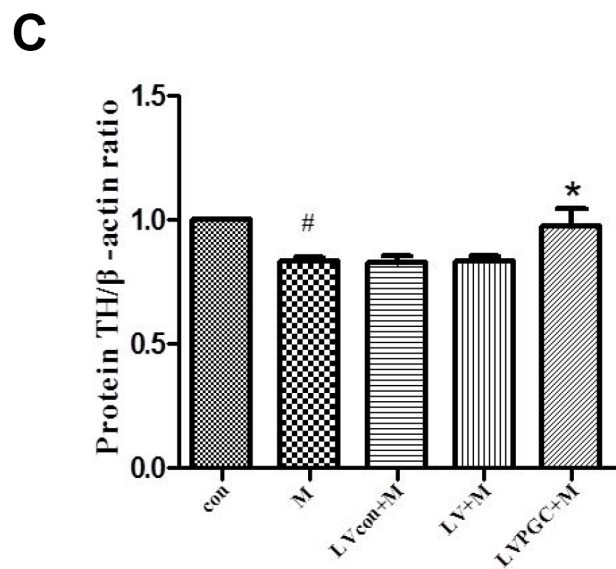
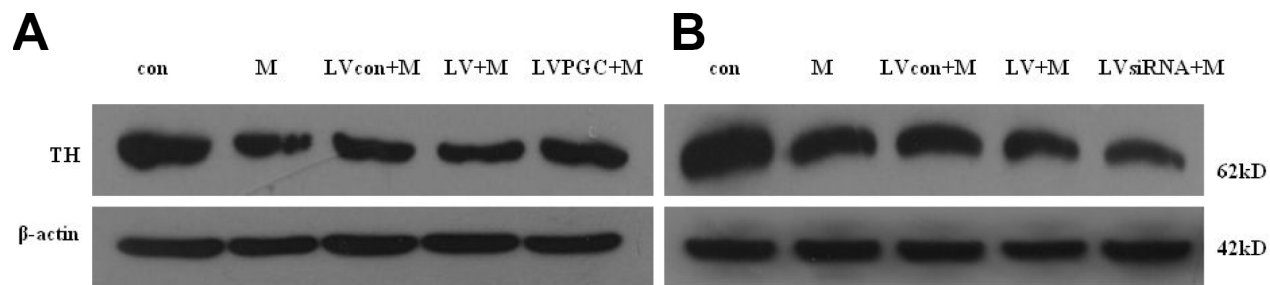
The success of the model can also be judged by the decrease in the dopaminergic neurons in the substantia nigra. Dopamine is an inhibitory and excitatory neurotransmitter in the central nervous system that is mainly synthesized by dopaminergic neurons in the substantia nigra of the midbrain and transported to the striatum via the substantia nigra–striatum pathway. TH, the key rate-limiting enzyme in the dopamine synthesis process, expression levels are consistent with the dopamine content in the nigrostriatal. Detecting the expression of TH can reflect the number and functional status of dopamine neurons, so this marker can be used to detect whether the MPTP-induced dopaminergic neurotoxicity model is successful [14]. The results of western blotting in the overexpression studies (Figure 4A, 4C) revealed that the TH levels in the SN were 16.70% lower in the M group than those in the con group ( $P < 0.05$ ), while those in the LVPGC+M group were

16.6% higher than those in the LV+M group ( $P < 0.05$ ). In the knockdown studies (Figure 4B, 4D), there was a significant decrease in TH expression in the M group compared to that in the con group (M vs. con, 39.31%,  $P < 0.001$ ). TH expression in the LVsiRNA+M group decreased by 38.61% compared with that in the LV+M group ( $P < 0.01$ ).

Immunohistochemical staining (Figure 4E) demonstrated positive brown TH staining in the SN. Dopamine-containing neurons were identified by their TH content. In the overexpression experiments (Figure 4F), the number of TH immunopositive cells in the SN of mice in the M group decreased by 36.13% compared to that in the con group ( $P < 0.01$ ), and the number in the LVPGC+M group increased by 32% compared to that in the LV+M group ( $P < 0.05$ ). In the knockdown studies (Figure 4G), TH expression levels in the M group decreased by 32.5% compared with those in the con group ( $P < 0.01$ ), and levels in the LVsiRNA+M group decreased by 13.95% compared with that in the



**Figure 3. Mouse behavioral changes before and after MPTP administration.** (A, B) The overall performance of mice in the rotarod test one day before injection and three days and six days after injection. The results of the three experiments are quantified as the means  $\pm$  SD. The groups were con (con group), M (MPTP group), LVcon+M (solvent of lentivirus+MPTP group), LV+M (lentivirus+MPTP group), LVPGC+M (LV-PGC-1 $\alpha$ +MPTP group), and LVsiRNA+M (LV-PGC-1 $\alpha$ siRNA+MPTP group); \* $P < 0.01$ , # $P < 0.05$  compared with before injection; ☆ $P < 0.01$  compared with the con group; \*\* $P < 0.01$  compared with the LV+M group.



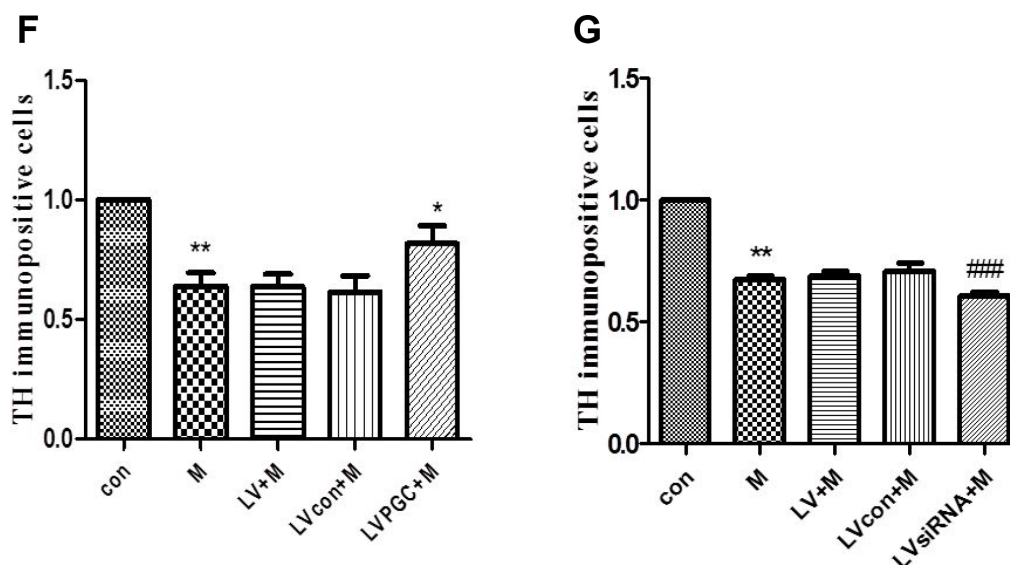


**Figure 4. Expression of TH and TH immunopositive cells in the substantia nigra of C57BL mice.** (A–D) TH protein expression detected using western blotting; (E–G) TH immunopositive cells (scale bar, 20  $\mu$ m, magnification,  $\times$ 400). Quantification of the results from the three experiments are represented as the means  $\pm$  SD. The groups were con (con group), M (MPTP group), LVcon+M (solvent of lentivirus+MPTP group), LV+M (lentivirus+MPTP group), LVPGC+M (LV-PGC-1 $\alpha$ +MPTP group), LVsiRNA+M (LV-PGC-1 $\alpha$ siRNA+MPTP group); \* $P$ <0.05, ### $P$ <0.01, ### $P$ <0.001, compared with the LV+M group; # $P$ <0.05, \*\*\* $P$ <0.001, \*\* $P$ <0.01 compared with the con group.

LVsiRNA+M group ( $P$ <0.001). By immunostaining, we found that TH-positive neurons showed a similar tendency to that of the TH protein in the SN. A prominent decrease in TH neuron loss induced by MPTP was observed. Taken together, the expression levels of PGC-1 $\alpha$  determine the TH protein level and the number of TH immunopositive cells.

#### Analysis of mitochondrial morphological changes after PGC-1 $\alpha$ intervention

PGC-1 $\alpha$  is one of the major regulators of mitochondrial biological origin and energy metabolism in cells. PGC-1 $\alpha$  can compensate for neuronal mitochondrial damage by increasing the number of mitochondria and protecting the morphological structure of mitochondria.

To examine whether PGC-1 $\alpha$  could protect mitochondria from MPTP intoxication, we investigated the morphological changes in mitochondria one week after MPTP administration using transmission electron microscopy (EM). (Figure 5A). There was an increased trend in the mitochondrial density in the LVPGC+M group and a decreasing trend in the M and LVsiRNA+M groups compared to that in the controls (Figure 5B). However, these trends did not reach statistical significance, possibly due to the small sample size and individual diversity within experimental animals. We found a significantly larger mitochondria area in the SN of LVPGC+M mice than in the control mice, which

could possibly be due to enhanced mitochondrial biogenesis by PGC-1 $\alpha$  (Figure 5C). There was no difference in the degree of mitochondrial branching between groups (Figure 5D).

#### SOD level in the substantia nigra

The neuroprotective effects of PGC-1 $\alpha$  may be related to the inhibition of ROS production, the increase in antioxidant enzymes and the protection of mitochondrial function. Superoxide dismutase (SOD) is the main antioxidant enzyme in mitochondria, and it can transform oxygen free radicals such as OH, H<sub>2</sub>, O<sub>2</sub> and other oxygen radicals into nontoxic hydrogen peroxide.

The WST-1 method was used to measure SOD concentration in SN homogenates from each group. In the overexpression studies (Figure 6A, Table 1), the levels of SOD induced by MPTP were 27.60% lower than those in the con group ( $P$ <0.01), while those in the LVPGC+M group were 17% higher than those in the LV+M group ( $P$ <0.01). In the knockdown studies (Figure 6B, Table 1), the SOD level showed a 21.15% decrease in the SN region after MPTP treatment compared with that in the con group ( $P$ <0.05). The SOD level in the LVsiRNA+M group was 29.26% lower than that in the LV+M group ( $P$ <0.05). The data above showed that MPTP treatment reduced total SOD activities, and the expression levels of PGC-1 $\alpha$  determined the SOD activities.

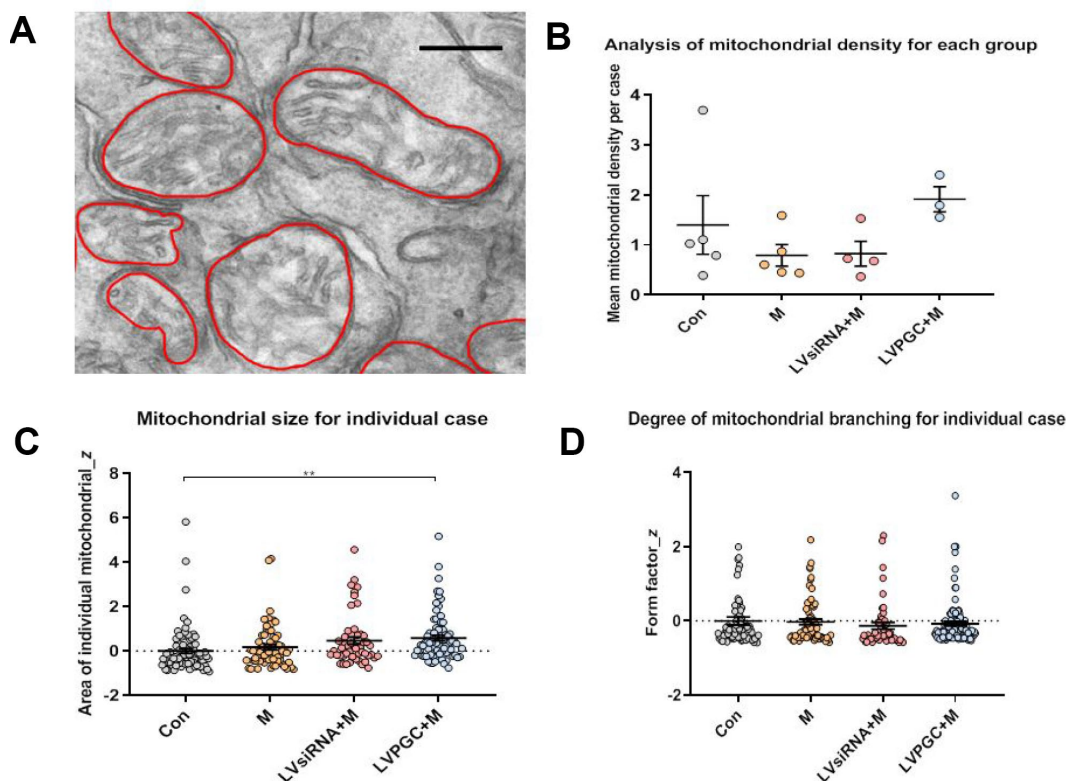


**Figure 5. Electron microscopy observation of the destruction of mitochondrial structure in SN neurons.** (A) Using electron microscopy (EM), SN images were collected from the group of con (number of mice, n=5), M (number of mice, n=5), LVPGC+M (number of mice, n=3), and LVsiRNA+M (number of mice, n=3). A total of 281 mitochondria were manually outlined and analyzed using QuPath software. Scale bar, 300 nm. (B) The average level of mitochondrial density was calculated for individual mice, which showed a higher trend in mitochondrial density in the LVPGC+M group and a lower trend in the M and LVsiRNA+M group compared to that in controls ( $P>0.05$ ). (C) Mitochondrial size in the LVPGC+M group was significantly increased compared with that in control mice ( $P>0.01$ ). (D) The degree of mitochondrial branching was also compared via the calculation of individual mitochondrial form factors.

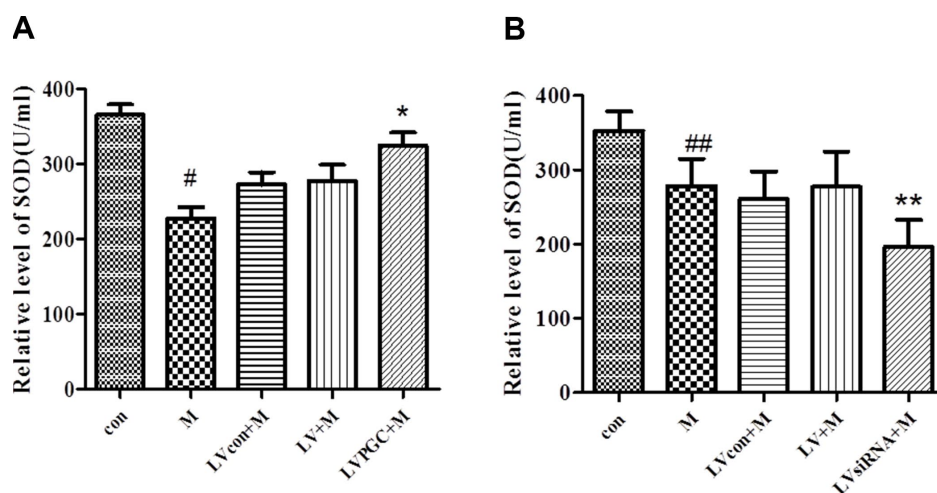


**Figure 6. Effects of PGC-1 $\alpha$  on the level of superoxide dismutase in a mouse model of Parkinson's disease (PD) induced by MPTP.** (A, B) Activity of SOD in the SN region of C57BL/6 mice with PGC-1 $\alpha$  overexpression or knockdown. Quantification of the results of the three experiments are presented as the means  $\pm$  SD. The groups were con (con group), M (MPTP group), LVcon+M (solvent of lentivirus+MPTP group), LV+M (lentivirus+MPTP group), LVPGC+M (LV-PGC-1 $\alpha$ +MPTP group), and LVsiRNA+M (LV-PGC-1 $\alpha$ siRNA+MPTP group); \* $P<0.01$ , \*\* $P<0.05$  compared with the LV+M group; # $P<0.01$ , ## $P<0.05$  compared with the con group.



**Table 1. SOD level shown as mean value ± standard deviation.**

Groups	con	M	LVcon+M	LV+M	LVPGC+M/ LVsiRNA+M
<b>SOD level (U/ml)</b>					
<b>Over-expression</b>	365.58±13.59	227.92±14.52	277.04±21.66	272.47±16.29	324.65±17.21
<b>Knock-down</b>	352.90±25.90	278.24±36.43	277.30±47.28	260.88±36.91	196.17±36.51

## DISCUSSION

The primary aim of the present study was to attain a better understanding of the role of PGC-1 $\alpha$  in the SN of an MPTP-treated dopaminergic neurotoxicity model, with a particular focus on beneficial effects against SN neuronal loss and mitochondrial dysfunction.

To establish an animal model with both dopaminergic neurotoxicity and mitochondrial dysfunction, a subacute MPTP treatment was implemented in C57BL/6 mice. The classic neurotoxin MPTP penetrates the blood-brain barrier and is then biotransformed by monoamine oxidase (MAO) to MPP<sup>+</sup> in the brain. MPP<sup>+</sup> specifically suppresses the activity of mitochondrial ETC complex I, leading to further ETC dysfunction, increased oxidative stress, and neuronal death. Behavioral performance and SN neuronal loss were investigated before and after the intervention to validate the model. Mice showed impaired rotarod performance three days after MPTP administration, including poor coordination and reduced endurance. However, this decrease was not observed on the sixth day after MPTP administration. It is interesting that the reduction in TH levels in the SN continued until the seventh day after MPTP administration, indicating that the recovery in rotarod performance was not due to the recovery of dopaminergic neurons. This result may be due to the existence of compensatory mechanisms, which first mask the existence of Parkinson's disease before the appearance of the first clinical symptoms and then delay the onset and aggravation of motor behavioral abnormalities. A number of factors are involved in these compensatory processes: the intrinsic properties of dopaminergic nigrostriatal neurons, neuronal plasticity, nonclassical DA volume transmission in the striatum, and different inputs to the SNc [15, 16]. Spontaneous recovery in behavioral performance has been reported in MPTP-treated mice [17]. In our study, performance on the third day may be due to acute cell injury after modeling, which leads to functional damage. After that, a compensatory mechanism is initiated that improves behavioral performance on the sixth day.

Human peroxisome proliferator-activated receptor  $\gamma$  (PPAR $\gamma$ ) coactivator 1 $\alpha$  (PGC-1 $\alpha$ ), together with PGC-1 $\beta$  and the PGC-related coactivator PRC, constitute the transcriptional coactivators of the peroxisome proliferator

activated receptor (PGC) family. To meet energy demands under different physiological and developmental conditions, PGC-1 $\alpha$  activity is activated via phosphorylation by a range of upstream signal factors. In recent rodent studies, the role of AMPK/PPAR/PGC-1 $\alpha$  signaling has been highlighted as having beneficial effects through the promotion of mitochondrial biogenesis, leading to neural protection [18, 19]. The overexpression of PGC-1 $\alpha$  rescued mitochondrial defects through an increase in mitochondrial biogenesis and the maintenance of mitochondrial morphology in neurons [20, 21]. Furthermore, PGC-1 $\alpha$  null mice showed increased vulnerability toward the neurodegenerative effects of MPTP. Consistent with the abovementioned results, in our study, knocking down PGC-1 $\alpha$  in the SN of MPTP-treated mice aggravated the toxic effects of MPTP, including a further loss of TH-positive neurons and impaired motor performance. It is notable that TH, the key rate-limiting enzyme involved in dopamine synthesis, was higher in the remaining neurons, indicating the potential role of PGC-1 $\alpha$  in the maintenance of neuronal function to balance dopamine content. This result could also explain the improved motor symptoms in the PGC-1 $\alpha$ -overexpressing mice.

The activation of PGC-1 $\alpha$  initiates the transcription cascade via the coactivation of several downstream regulators, including ERR $\alpha$  and mitofusin 1 and 2 (MFN1/MFN2), whose levels are altered due to mitochondrial fission and fusion. Increased PGC-1 $\alpha$  was reported to directly regulate mitochondrial dynamics, mainly by regulating the expression of fission and fusion genes in dopaminergic neurons of rat and human skeletal muscle [22, 23]. We observed enlarged mitochondria in PGC-1 $\alpha$ -overexpressing mice, possibly due to increased mitochondrial biogenesis and mitochondrial fusion. However, comparing mitochondrial branching did not show evidence to support the increase in mitochondrial fusion. The limitation of using two-dimensional EM analysis added extra difficulties in the interpretation of the mitochondrial morphological changes. Three-dimensional image acquisition and a larger sample size will be employed in the further investigation of mitochondrial morphology changes.

PGC-1 $\alpha$  is also associated with the generation of ROS and the expression of antioxidant enzymes [9, 24].

Mitochondrial DNA mutation, energy depletion, calcium overload, mitophagy, and apoptosis could be related to the overload of ROS [25]. This vicious circle is responsible for neuronal degeneration in the human midbrain [26]. PGC-1 $\alpha$  reduces ROS generation by regulating the expression and activity of ROS-detoxifying enzymes [27, 28]. SOD is one of the main antioxidant enzymes in mitochondria, converting oxygen radicals into nontoxic hydrogen peroxide. The overexpression of SOD reduced neurotoxicity in mouse SN neurons [29]. Conversely, mice deficient in CuZn-SOD and Mn-SOD genes were more susceptible to MPTP [30, 31]. PGC-1 $\alpha$  plays an important role in regulating the expression and activity of the mitochondrial antioxidant enzyme SOD2 in myocardial cells, endothelial cells and neurons [28, 32, 33]. Previously, we found that the overexpression of PGC-1 $\alpha$  reduced the release of cytochrome C and inhibited H<sub>2</sub>O<sub>2</sub> production in neuroblastoma [10]. In this study, the SOD level was lower after MPTP treatment in the SN of mice and was significantly increased in the SN of PGC-1 $\alpha$ -overexpressing mice. In contrast, an even lower level of SOD expression was observed in the SN after PGC-1 $\alpha$ -knockdown. It remains unclear whether this positive response originates from neurons themselves or from surrounding glial cells because there has been evidence of the ability of astrocytes to provide healthy mitochondria to neurons in response to increased oxidative stress [34].

## CONCLUSIONS

In a series of *ex vivo* studies, we validated the protective effects of PGC-1 $\alpha$  via manipulating its expression in human neuroblastoma cells with mitochondrial dysfunction [10, 11]. We then established similar mouse models to further assess the potential of PGC-1 $\alpha$  effects *in vivo*. In MPTP-treated mice, PGC-1 $\alpha$  inhibited MPTP-induced oxidative damage. This effect included the upregulation of SOD levels, the maintenance of mitochondrial structure, and improvements in SN neuron degeneration. The specific regulatory pathway involving PGC-1 $\alpha$  and other factors protecting C57BL/6 mice against MPTP warrants further study.

## MATERIALS AND METHODS

### Animals

Male C57BL/6 mice (weight 25–28 g, 14–16 weeks old, SLAC) were kept under a conventional 12-hour light–dark cycle in a temperature-controlled (20  $\pm$  2°C) room with free access to food and water.

Mice were randomly assigned to the following groups (n=24 per group): normal saline (NS) intraperitoneal

injection (i.p.) (con); MPTP i.p. (M); Solvent of lentivirus (lentivirus control) striatal injection + MPTP i.p. (LVcon+M); Lentivirus striatal injection + MPTP i.p. (LV+M); LV-PGC-1 $\alpha$  striatal injection + MPTP i.p. (LVPGC+M); and LV-PGC-1 $\alpha$ -siRNA striatal injection + MPTP i.p. (LVsiRNA+M). Intraperitoneal injections of MPTP/NS were conducted two weeks after lentivirus injection.

### Lentivirus production and stereotaxic injection

Lentivirus containing green fluorescent protein (GFP) and the PGC-1 $\alpha$  overexpression/siRNA constructs was engineered by GeneChem Technology. Viral stocks were thawed on ice and diluted to 2 $\times$ 10<sup>8</sup> TU/ml (LV-PGC-1 $\alpha$ ) and 5 $\times$ 10<sup>8</sup> TU/ml (LV-PGC-1 $\alpha$ -siRNA) with a lentivirus solvent. Mice were anesthetized with 10% chloral hydrate (400 mg/kg, i.p.) and positioned on a stereotaxic head frame (Stoelting). Solvent lentivirus (4 $\mu$ l), LV-PGC-1 $\alpha$  (4 $\mu$ l), and LV-PGC-1 $\alpha$ -siRNA (2.5 $\mu$ l) were stereotactically injected into the striatum at a speed of 0.25  $\mu$ l/min. Geometry-oriented coordinates of the mouse striatum were as follows: anterior, 0.5 mm; lateral, 2.2 mm; ventral, 3.4 mm; bregma as reference. After injection, the needle was left in place for an additional five minutes and slowly withdrawn (protocol adapted from [35]).

### MPTP treatment

Two weeks after striatal injections, mice were subjected to a total cumulative dose of 150 mg/kg MPTP i.p. (M0896, Sigma) for five consecutive days (30 mg/kg per day). The same amount of NS was injected into the con group to be used as the control. Whole brain samples were collected seven days after the last MPTP administration and were subdivided by different experimental procedures.

### Rotarod test

Rotarod testing was performed on an automated 5-lane rotarod unit (YLS-4C, Yiyang Science and Technology). All mice were pretrained for three consecutive days with two trials per day with 15-minute intervals between each trial. Formal tests were conducted before and on the third and sixth days after MPTP injections and were repeated three times per day with a minimum interval of 15 minutes between tests. The duration of each rotation was recorded, and the results were analyzed per the suggested protocol [12, 13, 36].

### Western blot analysis

Seven days after the last MPTP injection, mice were anesthetized as mentioned above and intracardially

perfused with 30 ml of 0.9% cold NS. Each SN was dissected on prechilled glass plates and lysed with RIPA lysis buffer (1% sodium deoxycholate, 0.1% SDS, 1 mM sodium orthovanadate, 50 mM sodium fluoride, and 1 mM EDTA). The supernatants were collected and processed using the standard Bradford assay (Beyotime).

Forty-five micrograms of denatured protein was loaded per lane and resolved by 8% SDS-PAGE (sodium dodecyl sulfate-polyacrylamide gel electrophoresis) for 90 minutes at 80 V. The separated proteins were transferred onto PVDF (polyvinylidene fluoride) membranes (Millipore, Carrigtwohill, Ireland) for 2 hours at 200 mA with Bradford reagent (Bio-Rad, Hercules, CA, USA). The membranes were blocked with 5% skimmed milk in 1×PBS (phosphate buffered saline) containing 0.05% Tween 20 (PBST) for 4 hours at room temperature. The following primary antibodies were used: anti-PGC-1 $\alpha$  1:1000 (EMD Millipore Billerica, MA, USA); anti-TH 1:1000 (1:1500 for suppression part) (EMD Millipore Billerica, MA, USA), anti-Actin (1:2000 Beyotime Company of Biotechnology Shanghai, China), which were contained in PBST and incubated at 4°C overnight. The membranes were washed three times in PBST for 10 minutes. Subsequently, the membranes were incubated for 1.5 hours in PBST containing secondary antibody conjugated to horseradish peroxidase (anti-rabbit IgG 1:2000 and anti-mouse IgG 1:2000, Beyotime Institute of Biotechnology, Shanghai, China). The immunoreactive bands were visualized and quantified using the enhanced chemiluminescence (ECL) detection kit (Millipore, USA).

### Quantitative real-time PCR

Total RNA extraction from SN homogenates was performed using the TRIzol method (Invitrogen). RNA was reverse-transcribed into cDNA using the RevertAid<sup>TM</sup> First Strand cDNA Synthesis Kit (K1621, Fermentas), and the amplification of cDNA was performed using the Fast Start Universal SYBR Green Master Mix (ROX) (Roche). Quantitative real-time PCR was carried out on the ABI Prism 7500 HT Sequence Detection System (Applied Biosystems) using the 5 $\beta$ -nuclease assay for the indicated genes and the housekeeping gene GAPDH. The level of mRNA was compared by quantifying the  $\Delta\Delta C_t$  value as described in [10, 11]. The primer sequences were as follows: LV-PGC-1 $\alpha$  forward, 5'-AAGCACTTCGGTCATCCCTGTC-3'; reverse, 5'-CGCACTTTCATCTTCACTGTCA TC-3'; LV-PGC-1 $\alpha$ -siRNA forward, 5'-AGCACTTCGTCATCCCTGTC-3'; reverse, 5'-GCACTTTCATCTTCACTGTCA TC-3' and GAPDH forward, 5'-ACGGCAAGTTCAACGGCACA G-3'; reverse, 5'-GAAGACGC CAGTAGACTCCACGAC-3'.

### Immunohistochemistry

For immunohistochemical staining, mice were perfused with 30 ml of 0.9% cold normal saline and 30 ml of 4% paraformaldehyde (PFA). The SN of each mouse was postfixed with 4% PFA for another 24 hours at 4°C and processed with 30% sucrose solution for 24–48 hours at 4°C. Tissues were then cryo-sectioned at 8  $\mu$ m thickness using a cryo-microtome (Leica).

Sections were dried at 37°C for an hour and immersed in 3% hydrogen peroxide (diluted in 100% v/v methanol) for 30 minutes. The sections were blocked with 3% normal goat serum for 30 minutes and incubated with rabbit anti-tyrosine hydroxylase (TH) antibody (1:400, Millipore) in a humidified chamber at 4°C overnight. This procedure was followed by incubation with biotinylated secondary antibody (anti-rabbit immunoglobulin G, 1:100) for one hour at room temperature. The sections were then labeled with streptavidin-peroxidase, 3,3-diaminobenzidine tetrahydrochloride dehydrate (DAB), and hematoxylin in sequence. After serial ethanol gradients (70%, 90% and 100% v/v) and xylene, the slides were mounted with Permount TM for storage. To measure the density of TH-positive cells in the substantia nigra, we performed counting as described by Bian M et al. [37]. One out of five sections and five sections were collected (n = 3 per group).

### Electron microscopy

The SN of each mouse was quickly dissected and processed with 3% glutaraldehyde, 1.5% paraformaldehyde, and 1.0 M PBS at 4°C per 24 hours each. This procedure was followed by postfixations in 1% osmium tetroxide and 1.5% potassium ferrocyanide at 4°C for 1.5 hours. After PBS washes, the samples were dehydrated in a graded series of ethanol (75%, 95%, 100% v/v) and embedded in an Epon-Araldite solution at 60°C for 72 hours. Sections were then cut at 100 nm thickness using an ultramicrotome (Leica) and imaged under an EM208 transmission electron microscope (Philips). For the analysis of EM images, individual mitochondria were manually outlined, and mitochondrial area and diameter were measured using QuPath software (v.0.1.2). The total mitochondrial area per snap was divided by snap area to represent a comparative mitochondrial density value. The mitochondrial form factor was calculated to show the degree of mitochondrial branching [38] based on the following equation:  $Form\ factor = Perimeter^2 / (4 \times \pi \times area)$ . All data were transformed into z scores and normalized based on controls.

## ELISA measurement of SOD activity

Each mouse SN was dissected on prechilled glass plates, weighed, and soaked in 0.9% cold NS to prepare 10% tissue homogenates. The supernatants were collected after a ten minute centrifugation (3000 rpm) at 4°C and stored at -80°C. SOD activity was determined using the Superoxide Dismutase (SOD) WST-1 assay kit (Nanjing Jiancheng Bioengineering).

## Statistical analysis

All quantitative data were collected from at least three independent experiments. Data were analyzed using SPSS 17.0 statistical software. Real-time PCR data (Ct values) were converted into the  $2^{-\Delta\Delta C_t}$  format for statistical analysis. Differences between the mean values were analyzed using one-way analysis of variance (ANOVA), and  $P < 0.05$  was considered significant.

## Abbreviations

PGC-1 $\alpha$ : Peroxisome proliferator-activated receptor- $\gamma$  coactivator-1 $\alpha$ ; MPTP: 1-methyl-4-phenyl-1,2,3,6-tetrahydropyridine; SOD: Superoxide Dismutase; TH: Tyrosine Hydroxylase; SN: Substantia Nigra; LV: Lentivirus.

## AUTHOR CONTRIBUTIONS

Qinyong Ye conceived and supervised the study. Yingqing Wang and Chun Chen completed the experiments and writing. Wanling Huang and Maoxin Huang helped with the cryodissection of midbrain tissue, Juhua Wang help with the PCR data analysis. Operation of animal experiment is supervised by Xiaochun Chen.

## ACKNOWLEDGMENTS

We thank En Huang, Jing Zhang, Xiaoman Dai, Hongbin Chen for expert technical assistance. This work was supported by the National Natural Science Fund of China (General Program No. 81271414 and No.81671265).

## CONFLICTS OF INTEREST

The authors declare that they have no conflicts of interests.

## FUNDING

This work was supported by the National Natural Science Fund of China (General Program No. 81271414 and No.81671265).

## REFERENCES

1. Mizuno Y, Ohta S, Tanaka M, Takamiya S, Suzuki K, Sato T, Oya H, Ozawa T, Kagawa Y. Deficiencies in complex I subunits of the respiratory chain in Parkinson's disease. *Biochem Biophys Res Commun.* 1989; 163:1450–55.  
[https://doi.org/10.1016/0006-291X\(89\)91141-8](https://doi.org/10.1016/0006-291X(89)91141-8)  
PMID:2551290
2. Schapira AH, Cooper JM, Dexter D, Clark JB, Jenner P, Marsden CD. Mitochondrial complex I deficiency in Parkinson's disease. *J Neurochem.* 1990; 54:823–27.  
<https://doi.org/10.1111/j.1471-4159.1990.tb02325.x>  
PMID:2154550
3. Beal MF. Experimental models of Parkinson's disease. *Nat Rev Neurosci.* 2001; 2:325–34.  
<https://doi.org/10.1038/35072550>  
PMID:11331916
4. Puigserver P, Wu Z, Park CW, Graves R, Wright M, Spiegelman BM. A cold-inducible coactivator of nuclear receptors linked to adaptive thermogenesis. *Cell.* 1998; 92:829–39.  
[https://doi.org/10.1016/S0092-8674\(00\)81410-5](https://doi.org/10.1016/S0092-8674(00)81410-5)  
PMID:9529258
5. Lin J, Wu H, Tarr PT, Zhang CY, Wu Z, Boss O, Michael LF, Puigserver P, Isotani E, Olson EN, Lowell BB, Bassel-Duby R, Spiegelman BM. Transcriptional co-activator PGC-1 alpha drives the formation of slow-twitch muscle fibres. *Nature.* 2002; 418:797–801.  
<https://doi.org/10.1038/nature00904>  
PMID:12181572
6. Zheng B, Liao Z, Locascio JJ, Lesniak KA, Roderick SS, Watt ML, Eklund AC, Zhang-James Y, Kim PD, Hauser MA, Grünblatt E, Moran LB, Mandel SA, et al, and Global PD Gene Expression (GPEx) Consortium. PGC-1 $\alpha$ , a potential therapeutic target for early intervention in Parkinson's disease. *Sci Transl Med.* 2010; 2:52ra73.  
<https://doi.org/10.1126/scitranslmed.3001059>  
PMID:20926834
7. Liang H, Ward WF, Jang YC, Bhattacharya A, Bokov AF, Li Y, Jernigan A, Richardson A, Van Remmen H. PGC-1 $\alpha$  protects neurons and alters disease progression in an amyotrophic lateral sclerosis mouse model. *Muscle Nerve.* 2011; 44:947–56.  
<https://doi.org/10.1002/mus.22217> PMID:22102466
8. Jiang H, Kang SU, Zhang S, Karuppagounder S, Xu J, Lee YK, Kang BG, Lee Y, Zhang J, Pletnikova O, Troncoso JC, Pirooznia S, Andrabi SA, et al. Adult Conditional Knockout of PGC-1 $\alpha$  Leads to Loss of Dopamine Neurons. *eNeuro.* 2016; 3.  
<https://doi.org/10.1523/ENEURO.0183-16.2016>  
PMID:27622213

9. Mudò G, Mäkelä J, Di Liberto V, Tselykh TV, Olivieri M, Piepponen P, Eriksson O, Mälkiä A, Bonomo A, Kairisalo M, Aguirre JA, Korhonen L, Belluardo N, Lindholm D. Transgenic expression and activation of PGC-1 $\alpha$  protect dopaminergic neurons in the MPTP mouse model of Parkinson's disease. *Cell Mol Life Sci.* 2012; 69:1153–65.  
<https://doi.org/10.1007/s00018-011-0850-z>  
PMID:21984601
10. Ye Q, Huang W, Li D, Si E, Wang J, Wang Y, Chen C, Chen X. Overexpression of PGC-1 $\alpha$  Influences Mitochondrial Signal Transduction of Dopaminergic Neurons. *Mol Neurobiol.* 2016; 53:3756–3770.  
<https://doi.org/10.1007/s12035-015-9299-7>  
PMID:26141122
11. Ye Q, Chen C, Si E, Cai Y, Wang J, Huang W, Li D, Wang Y, Chen X. Mitochondrial Effects of PGC-1 $\alpha$  Silencing in MPP(+) Treated Human SH-SY5Y Neuroblastoma Cells. *Front Mol Neurosci.* 2017; 10:164.  
<https://doi.org/10.3389/fnmol.2017.00164>  
PMID:28611589
12. Rozas G, Guerra MJ, Labandeira-García JL. An automated rotarod method for quantitative drug-free evaluation of overall motor deficits in rat models of parkinsonism. *Brain Res Brain Res Protoc.* 1997; 2:75–84.  
[https://doi.org/10.1016/S1385-299X\(97\)00034-2](https://doi.org/10.1016/S1385-299X(97)00034-2)  
PMID:9438075
13. Brooks SP, Trueman RC, Dunnett SB. Assessment of Motor Coordination and Balance in Mice Using the Rotarod, Elevated Bridge, and Footprint Tests. *Curr Protoc Mouse Biol.* 2012; 2:37–53.  
<https://doi.org/10.1002/9780470942390.mo110165>  
PMID:26069004
14. Ichitani Y, Okamura H, Nakahara D, Nagatsu I, Iyata Y. Biochemical and immunocytochemical changes induced by intrastriatal 6-hydroxydopamine injection in the rat nigrostriatal dopamine neuron system: evidence for cell death in the substantia nigra. *Exp Neurol.* 1994; 130:269–78.  
<https://doi.org/10.1006/exnr.1994.1205>  
PMID:7867756
15. Bezdard E, Gross CE. Compensatory mechanisms in experimental and human parkinsonism: towards a dynamic approach. *Prog Neurobiol.* 1998; 55:93–116.  
[https://doi.org/10.1016/S0301-0082\(98\)00006-9](https://doi.org/10.1016/S0301-0082(98)00006-9)  
PMID:9618745
16. Zhang QS, Heng Y, Mou Z, Huang JY, Yuan YH, Chen NH. Reassessment of subacute MPTP-treated mice as animal model of Parkinson's disease. *Acta Pharmacol Sin.* 2017; 38:1317–28.  
<https://doi.org/10.1038/aps.2017.49> PMID:28649132
17. Weihmuller FB, Hadjiconstantinou M, Bruno JP. Dissociation between biochemical and behavioral recovery in MPTP-treated mice. *Pharmacol Biochem Behav.* 1989; 34:113–17.  
[https://doi.org/10.1016/0091-3057\(89\)90362-6](https://doi.org/10.1016/0091-3057(89)90362-6)  
PMID:2696981
18. Kim E, Park M, Jeong J, Kim H, Lee SK, Lee E, Oh BH, Namkoong K. Cholinesterase Inhibitor Donepezil Increases Mitochondrial Biogenesis through AMP-Activated Protein Kinase in the Hippocampus. *Neuropsychobiology.* 2016; 73:81–91.  
<https://doi.org/10.1159/000441522>  
PMID:27002982
19. Yerra VG, Areti A, Kumar A. Adenosine Monophosphate-Activated Protein Kinase Abates Hyperglycaemia-Induced Neuronal Injury in Experimental Models of Diabetic Neuropathy: Effects on Mitochondrial Biogenesis, Autophagy and Neuroinflammation. *Mol Neurobiol.* 2017; 54:2301–12.  
<https://doi.org/10.1007/s12035-016-9824-3>  
PMID:26957299
20. Wareski P, Vaarmann A, Choubey V, Safiulina D, Liiv J, Kuum M, Kaasik A. PGC-1 $\alpha$  and PGC-1 $\beta$  regulate mitochondrial density in neurons. *J Biol Chem.* 2009; 284:21379–85.  
<https://doi.org/10.1074/jbc.M109.018911>  
PMID:19542216
21. Rodríguez-Martínez E, Martínez F, Espinosa-García MT, Maldonado P, Rivas-Arancibia S. Mitochondrial dysfunction in the hippocampus of rats caused by chronic oxidative stress. *Neuroscience.* 2013; 252:384–95.  
<https://doi.org/10.1016/j.neuroscience.2013.08.018>  
PMID:23988432
22. Dabrowska A, Venero JL, Iwasawa R, Hankir MK, Rahman S, Boobis A, Hajji N. PGC-1 $\alpha$  controls mitochondrial biogenesis and dynamics in lead-induced neurotoxicity. *Aging (Albany NY).* 2015; 7:629–47.  
<https://doi.org/10.18632/aging.100790>  
PMID:26363853
23. Cartoni R, Léger B, Hock MB, Praz M, Crettenand A, Pich S, Ziltener JL, Luthi F, Dériaz O, Zorzano A, Gobelet C, Kralli A, Russell AP. Mitofusins 1/2 and ERR $\alpha$  expression are increased in human skeletal muscle after physical exercise. *J Physiol.* 2005; 567:349–58.  
<https://doi.org/10.1113/jphysiol.2005.092031>  
PMID:15961417
24. Scarpulla RC, Vega RB, Kelly DP. Transcriptional integration of mitochondrial biogenesis. *Trends Endocrinol Metab.* 2012; 23:459–66.  
<https://doi.org/10.1016/j.tem.2012.06.006>  
PMID:22817841

25. Keane PC, Kurzawa M, Blain PG, Morris CM. Mitochondrial dysfunction in Parkinson's disease. *Parkinsons Dis.* 2011; 2011:716871. <https://doi.org/10.4061/2011/716871> PMID:[21461368](https://pubmed.ncbi.nlm.nih.gov/21461368/)
26. Esteves AR, Arduíno DM, Swerdlow RH, Oliveira CR, Cardoso SM. Oxidative stress involvement in alpha-synuclein oligomerization in Parkinson's disease cybrids. *Antioxid Redox Signal.* 2009; 11:439–48. <https://doi.org/10.1089/ARS.2008.2247> PMID:[18717628](https://pubmed.ncbi.nlm.nih.gov/18717628/)
27. Eschbach J, von Einem B, Müller K, Bayer H, Scheffold A, Morrison BE, Rudolph KL, Thal DR, Witting A, Weydt P, Otto M, Fauler M, Liss B, et al. Mutual exacerbation of peroxisome proliferator-activated receptor  $\gamma$  coactivator 1 $\alpha$  deregulation and  $\alpha$ -synuclein oligomerization. *Ann Neurol.* 2015; 77:15–32. <https://doi.org/10.1002/ana.24294> PMID:[25363075](https://pubmed.ncbi.nlm.nih.gov/25363075/)
28. St-Pierre J, Drori S, Uldry M, Silvaggi JM, Rhee J, Jäger S, Handschin C, Zheng K, Lin J, Yang W, Simon DK, Bachoo R, Spiegelman BM. Suppression of reactive oxygen species and neurodegeneration by the PGC-1 transcriptional coactivators. *Cell.* 2006; 127:397–408. <https://doi.org/10.1016/j.cell.2006.09.024> PMID:[17055439](https://pubmed.ncbi.nlm.nih.gov/17055439/)
29. Andrews AM, Ladenheim B, Epstein CJ, Cadet JL, Murphy DL. Transgenic mice with high levels of superoxide dismutase activity are protected from the neurotoxic effects of 2'-NH<sub>2</sub>-MPTP on serotonergic and noradrenergic nerve terminals. *Mol Pharmacol.* 1996; 50:1511–19. PMID:[8967972](https://pubmed.ncbi.nlm.nih.gov/8967972/)
30. Andreassen OA, Ferrante RJ, Klivenyi P, Klein AM, Dedeoglu A, Albers DS, Kowall NW, Beal MF. Transgenic ALS mice show increased vulnerability to the mitochondrial toxins MPTP and 3-nitropropionic acid. *Exp Neurol.* 2001; 168:356–63. <https://doi.org/10.1006/exnr.2001.7627> PMID:[11259123](https://pubmed.ncbi.nlm.nih.gov/11259123/)
31. Andreassen OA, Ferrante RJ, Dedeoglu A, Albers DW, Klivenyi P, Carlson EJ, Epstein CJ, Beal MF. Mice with a partial deficiency of manganese superoxide dismutase show increased vulnerability to the mitochondrial toxins malonate, 3-nitropropionic acid, and MPTP. *Exp Neurol.* 2001; 167:189–95. <https://doi.org/10.1006/exnr.2000.7525> PMID:[11161607](https://pubmed.ncbi.nlm.nih.gov/11161607/)
32. Valle I, Alvarez-Barrientos A, Arza E, Lamas S, Monsalve M. PGC-1 $\alpha$  regulates the mitochondrial antioxidant defense system in vascular endothelial cells. *Cardiovasc Res.* 2005; 66:562–73. <https://doi.org/10.1016/j.cardiores.2005.01.026> PMID:[15914121](https://pubmed.ncbi.nlm.nih.gov/15914121/)
33. Lu Z, Xu X, Hu X, Fassett J, Zhu G, Tao Y, Li J, Huang Y, Zhang P, Zhao B, Chen Y. PGC-1  $\alpha$  regulates expression of myocardial mitochondrial antioxidants and myocardial oxidative stress after chronic systolic overload. *Antioxid Redox Signal.* 2010; 13:1011–22. <https://doi.org/10.1089/ars.2009.2940> PMID:[20406135](https://pubmed.ncbi.nlm.nih.gov/20406135/)
34. Hayakawa K, Esposito E, Wang X, Terasaki Y, Liu Y, Xing C, Ji X, Lo EH. Transfer of mitochondria from astrocytes to neurons after stroke. *Nature.* 2016; 535:551–55. <https://doi.org/10.1038/nature18928> PMID:[27466127](https://pubmed.ncbi.nlm.nih.gov/27466127/)
35. Cetin A, Komai S, Eliava M, Seeburg PH, Osten P. Stereotaxic gene delivery in the rodent brain. *Nat Protoc.* 2006; 1:3166–73. <https://doi.org/10.1038/nprot.2006.450> PMID:[17406580](https://pubmed.ncbi.nlm.nih.gov/17406580/)
36. Hamm RJ, Pike BR, O'Dell DM, Lyeth BG, Jenkins LW. The rotarod test: an evaluation of its effectiveness in assessing motor deficits following traumatic brain injury. *J Neurotrauma.* 1994; 11:187–96. <https://doi.org/10.1089/neu.1994.11.187> PMID:[7932797](https://pubmed.ncbi.nlm.nih.gov/7932797/)
37. Bian M, Liu J, Hong X, Yu M, Huang Y, Sheng Z, Fei J, Huang F. Overexpression of parkin ameliorates dopaminergic neurodegeneration induced by 1-methyl-4-phenyl-1,2,3,6-tetrahydropyridine in mice. *PLoS One.* 2012; 7:e39953. <https://doi.org/10.1371/journal.pone.0039953> PMID:[22792139](https://pubmed.ncbi.nlm.nih.gov/22792139/)
38. Mortiboys H, Thomas KJ, Koopman WJ, Klaffke S, Abou-Sleiman P, Olpin S, Wood NW, Willems PH, Smeitink JA, Cookson MR, Bandmann O. Mitochondrial function and morphology are impaired in parkin-mutant fibroblasts. *Ann Neurol.* 2008; 64:555–65. <https://doi.org/10.1002/ana.21492> PMID:[19067348](https://pubmed.ncbi.nlm.nih.gov/19067348/)